Thermal Stability and Degradation Kinetics of Paraffin Wax and Graphene-Enhanced Phase Change Materials Analyzed through Thermogravimetry, Kinetics, and Machine Learning

K. Pavan Kumar[1,2,*], T. V. K. Bhanu Prakash[3], and Aditya Mukherjee[4]

ARTICLE INFO

Article history:
Received: 2 July 2025
Revised: 30 Juanary 2025
Accepted: 21 February 2026
Online: 20 July 2026

Keywords:
Paraffin wax
Phase change materials
Graphene nanoplatelets
Analytic hierarchy process
Thermogravimetric analysis
Machine learning models

ABSTRACT

The thermal stability and degradation kinetics of paraffin wax–based phase change materials (PCMs) enhanced with graphene nanoplatelets (GNP, 0.25–1.0 wt%) are investigated using thermogravimetric analysis, model-free kinetic methods, and data-driven prediction. Paraffin wax was selected as the base PCM through an Analytic Hierarchy Process considering thermal reliability, cost, and energy storage relevance. Non-isothermal thermogravimetric experiments were carried out at heating rates between 10 and 25 °C/min, and activation energies were evaluated using the Kissinger–Akahira–Sunose, Flynn–Wall–Ozawa, and Starink approaches. The results show a clear improvement in thermal stability with GNP addition, where the activation energy increases from 69.34 kJ/mol for pure paraffin to 85.79 kJ/mol for the composite containing 1 wt% GNP, corresponding to an enhancement of approximately 23.7%. The variation of activation energy with conversion degree (α = 0.2–0.8) indicates the presence of multi-step degradation mechanisms associated with thermal barrier effects and paraffin–graphene interfacial interactions. To reduce experimental effort, machine-learning regression models were developed to predict mass-loss behavior as a function of temperature, heating rate, and GNP concentration. Among the evaluated models, random forest regression showed the highest accuracy (R^2 = 0.999, RMSE = 0.0003), closely matching experimental observations. The combined kinetic–machine-learning framework offers a practical and quantitative approach for the design and optimization of nano-enhanced PCMs for medium-temperature thermal energy storage applications.

1. INTRODUCTION

Phase Change Materials (PCMs), particularly paraffin wax, are key components to energy saving and temperature control in the different engineering systems due to their capacity of heat storage and heat release during their solid-liquid phase change [1], [2]. Nevertheless, the biggest problem that hinders the extensive use of organic PCMs in medium- and high-temperature thermal energy storage (TES) situations is their low thermal stability and weak thermal conductivity which are intrinsic features of these materials [3]. Their deterioration will be slowed down but still, their vulnerability to thermal decomposition during long cycles of operation is a big issue that has not been solved yet [4], [5].

Enhanced PCMs with Nano-Additives

Nano-additive integration has proven essential for overcoming organic PCM limitations. The studies indicate that the use of carbon-based nanomaterials and metal oxides with a high surface area can have a significant effect on the thermal conductivity and, what is very important, can greatly increase the thermal stability of PCMs [6]–[10]. An example is the research results, which demonstrate that T_iO_2 and MWCNTs are able to raise both conductivity and degradation temperatures, thus confirming the advantages of NEPCMs for the situations where high durability is needed [11]–[15]. The attention is still on Graphene Nanoplatelets (GNP) because of their outstanding thermal properties.

Multi-Criteria Decision-Making (MCDM) in PCM Selection

Selecting the optimal PCM/additive composite for high-performance applications requires a systematic decision-making process. Multi-Criteria Decision-Making (MCDM) instruments like the Analytic Hierarchy Process (AHP) help in evaluating several technical criteria (e.g., latent heat, density, cost, and thermal stability) to identify the material

[1]*Research Scholar, Andhra University, Visakhapatnam, 530003, AP, India,*
[2]*MVGR College of Engineering(A), Vizianagram, 535005, AP, India.*
[3]*Department of Marine Engineering, 1Andhra University, Visakhapatnam, 530003, AP, India.*
[4]*Department of Chemical Engineering, GVP College of Engineering, Visakhapatnam—530048, AP, India.*
**Corresponding author:* K. Pavan Kumar; Email: pavankmech@gmail.com.

combination with the greatest potential [16]–[19]. The paraffin-GNP system selection for this research was lead by a preliminary AHP analysis, thereby providing the rationale for the detailed experimental and kinetic study reported here.

Kinetic Analysis and Research Gap

Thermogravimetric Analysis (TGA) is typically used to carry out thermal stability evaluation. TGA gives characteristic temperatures (T_{onset}, T_{max}) but a large number of NEPCM-related publications, as well as the very first work on GNP-paraffin, only report these descriptive TGA results [7], [10]. Such an approach is not thorough as it does not result in the derivation of the kinetic parameters, i.e. Activation Energy (E_a) dependent on conversion rate (α), which is indispensable for lifetime estimation and gaining the insight of the degradation processes at the molecular level. The complete implementation of model-free isoconversional methods (KAS, FWO, Starink) is required to bridge this gap and deliver dependable kinetic data [20], [21].

Machine Learning in Thermal Degradation Prediction

In order to supplement bench and kinetic studies, ML models are getting more and more utilized in materials science for the prediction of properties that have not been measured experimentally. The creation of predictive models, e.g., the Random Forest Regressor, for complicated thermal processes (such as TGA mass loss) is an extremely fast and inexpensive instrument for the local composite formulation and quality control standardization. Thermal stability can thus be conveniently ensured via this method of newly developed composites, which in turn results in the saving of a great amount of experimental works [22] [23].

Recent studies have demonstrated that machine-learning regression models, particularly tree-based methods, can accurately predict thermophysical properties of polymer composites by learning complex, nonlinear relationships from experimental datasets, thereby reducing reliance on empirical correlations [44]. Recent reviews on graphene-based phase-change composites highlight their superior thermal conductivity, improved phase stability, and multifunctional energy conversion capability, reinforcing the suitability of graphene nanomaterials for enhancing the performance and durability of PCM systems [45],[46].

This research addresses critical knowledge gaps through comprehensive multi-level examination of the thermal stability and the decay of the paraffin wax enhanced with graphite nanoplatelets (GNP), which is a material that has been prioritized through the initial AHP selection. We have three significant methodologies that are combined in our work to generate comprehensive knowledge:

i) Fundamental Thermal Stability and Kinetic Analysis: Non-isothermal TGA is performed at different heating rates to locate the thermal decomposition characteristics accurately. After that, model-free kinetic methods (Kissinger-Akahira-Sunose (KAS), Flynn-Wall-Ozawa (FWO), and Starink) are employed to find the Activation Energy (E_a) correspondingly to the conversion rate (α). The main point of this process is mechanistic insight to provide explanation for GNP stabilizing effect that is necessary for lifetime prediction of material.

ii) Mechanistic Interpretation of GNP Effect: We offer a mechanism by which GNP leads to an increase in E_a concentration, in particular, explaining how the E_a dependence on α is linked to the limiting of polymer chain due to GNP-paraffin interaction.

iii) Machine Learning (ML) Predictive Modeling: Based on the TGA data (Temperature, Heating Rate, and GNP Concentration), a Random Forest Regressor model has been designed to serve as an extremely accurate, non-experimental tool for Mass Loss percentage prediction. The ML model of this kind is indispensable because it allows the thermal stability of newly developed composites to be quickly checked, thus the selection of materials can be done in an optimal way, and extensive experimental works can be saved.

The main points of this paper are the quantitative demonstration of the stabilizing effect of GNP on paraffin wax, the mechanistic confirmation of this stability by means of the advanced kinetic analysis, and the creation of a high-precision predictive ML model ($R^2 > 0.98$) for the thermal degradation of composites.

Novelty and Contribution

Previous research has, over time, separate stages, addressed TGA kinetics or machine-learning-based PCM modeling; however, the present study is the first one that has systematically combined both approaches for graphene-enhanced paraffin wax systems. The foremost novelties are:

i. Concentration-dependent kinetic analysis (0–1.0 wt% GNP) by three isoconversional models over various heating rates;
ii. Conversion-dependent activation energy interpretation pointing multi-step degradation mechanisms; and
iii. The establishment of a high-accuracy Random Forest model ($R^2 = 0.999$) for a prompt thermal stability prediction without a time-consuming trial.

This integrated framework, which mechanistically understands and predictively is capable, is different from TGA descriptive studies or purely computational ML approaches in that it uniquely combines the two to empower quantitative design optimization of nano-enhanced PCMs.

The rest of the article is structured as follows: Section 2 describes the Materials and Methods employed, the initial AHP selection process, TGA procedure, kinetic models, and

the Machine Learning methodology. Section 3 shows the TGA and Kinetic Results. Section 4 displays the Machine Learning Prediction Results. Section 5 is a comprehensive Discussion that compares the findings with the literature and provides a mechanistic interpretation. Lastly, Section 6 outlines the Conclusion, new contributions, and future work directions.

2. MULTI-CRITERIA DECISION-MAKING (MCDM) FOR PCM SELECTION (AHP)

This study began with systematic selection of the optimal base Phase Change Material (PCM) for a medium-temperature Thermal Energy Storage (TES) system. The Analytic Hierarchy Process (AHP) was the indispensable Multi-Criteria Decision-Making (MCDM) instrument that helped the evaluation and ranking of candidate PCMs to be done based on numerous quantitative and qualitative criteria [6], [7]. The AHP pre-experimental analysis served as validation to ensure to make sure the selected material was the ideal platform for subsequent nano-enhancement and kinetic study.

Seven critical criteria, that involved latent heat, cost, thermal reliability, and environmental impact among others, were used to evaluate six commercial PCMs (Eicosane, Octadecane, Myristic Alcohol, Paraffin Wax, PEG 1000, and Lauric Acid) [7]–[10]. The AHP results, which are briefed in Table 1, very clearly ranked Paraffin Wax as the best choice (Weight = 0.333) for the target application.

In a brief comparison, Eicosane was leading in thermal conductivity, however, the advantage of Paraffin Wax in terms of cost, specific heat, and overall thermal reliability was enough to keep it at the top of the list for Rank 1 [11], [12]. So, the AHP outcome was the main driver of the experimental design: hence, for the in-depth TGA and kinetic analysis, Graphene Nanoplatelets (GNP) enhanced Paraffin Wax was the decided fundamental base material.

Table 1. Ranking of Phase Change Material (PCM) Alternatives Based on Overall Weights

Option Name	Overall alternative weights	Rank
Eicosane	0.219	2
Octadecane	0.096	5
Myristic Alcohol	0.096	6
Paraffin Wax	**0.333**	**1**
PEG 1000	0.14	3
Lauric Acid	0.116	4

3. KINETIC ANALYSIS METHODOLOGY

Thermogravimetric Analysis (TGA) was employed to determine the thermal stability of pure paraffin and GNP-enhanced composites through the measurement of degradation temperatures and rates. The TGA data obtained from experiments at different heating rates were also utilized to find the materials' degradation kinetics [16],[17].

3.1 Model-Free Kinetic Analysis

The thermal degradation kinetics were derived from three model-free isoconversional methods: the Kissinger-Akahira-Sunose (KAS), the Flynn-Wall-Ozawa (FWO), and the Starink methods. These integral methods serve to find the apparent Activation Energy (E_a) depending on the conversion rate (α) without giving the reaction mechanism in advance, which is very significant for complicated solid-state degradation [18], [19], [20]. The operations, which are working equations, come from the integral form of the Arrhenius equation and are shown here.

KAS Method [21], [22]:

$$ln\left(\frac{\beta}{T^2}\right) = ln\left(\frac{AR}{E_a}\right) - \frac{E_a}{RT} \quad (1)$$

FWO Method [22], [24]:

$$log(\beta) = log\frac{AE_a}{R} - log\big(g(\alpha)\big) - 2.315 - \frac{0.4567E_a}{RT} \quad (2)$$

Starink Method [25], [27]:

$$log\left(\frac{\beta}{T^{1.92}}\right) = log\left(\frac{AE_a}{R}\right) - \frac{E_a}{2.303\,RT} \quad (3)$$

where, β is the heating rate, T is the absolute temperature, and. For each method, the E_a is calculated from the slope of the linear plot of the left-hand side versus 1/T at a fixed value of α.

3.2 Machine Learning Methodology

The thermal stability dataset was used as input for different Machine Learning (ML) regression models with the aim of creating a non-experimental, highly accurate prediction tool for mass loss. As a result of its strength against overfitting and the usefulness of its features in modeling the non-linear relationship typical for TGA data, Random Forest Regression was chosen as the main model [28]-[36]. Moreover, to the Linear and Polynomial Regression models, which are of a simpler nature, were also utilized for the comparative analysis purpose.

Random Forest Regression is a machine learning technique that aggregates the outputs of multiple decision trees to forecast continuous variables. In Random Forest, each of the T decision trees is constructed on a random subset of the original dataset that will be used for prediction. The probability of overfitting a single decision tree can be reduced by random selection of data features. This allows you to use a random set of features for the decision split. [36]–[43] The mean of f(x) will be the same as the average of the T decision trees' predictions from earlier in the formula. That is, if $f_i(x)$ is the prediction function for the ith tree, then:

$$f(x) = \frac{1}{T}\sum_{i=1}^{T} f_i(x) \quad (4)$$

After setting up the methodological groundwork—AHP-based material selection (Section 2) and model-free kinetic analysis supplemented by machine learning (Section 3)—the next section details the experimental implementation starting with the sample preparation protocols that assure reproducible GNP dispersion, and continuing with systematic TGA characterization and kinetic parameter determination.

4. RESULT AND DISCUSSION

4.1 Experimentation Preparation of Sample

Paraffin wax is a common phase change material (PCM) for thermal energy storage, producing thermal energy storage responses due to latent heat at high levels. However, paraffin wax has low thermal conductivity, and overall, low thermal conductivity is a limitation in different forms of heat transfer. To minimize the effects of low thermal conductivity, additives can be added to PCMs. In particular, when using nano-additives like graphene nanoplatelets (GNPs) the thermal properties of PCMs are increased. Nano-additives can impart properties that lead to improved thermal dissipation and limit the thermal degradation of PCMs [19]. The preparation process has been illustrated, in Figure-1, which begins by mixing pure paraffin wax with GNPs to improve the thermal efficiency of this composite.

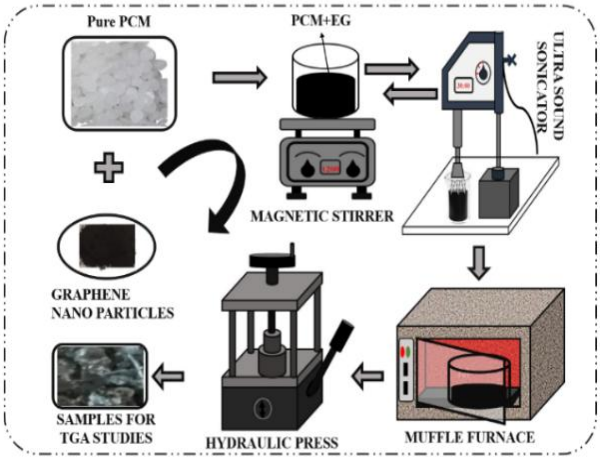

Fig. 1. Preparation Process of Paraffin PCM Enhanced with Graphene Nanoplatelets.

Initially, the GNPs are dispersed with a coarse technique into paraffin wax using a magnetic stirrer. To achieve finer GNP distribution and uniform coating of nano-additive throughout the PCM, the paraffin wax and the GNPs must be passed through ultrasonic sonication first, which is essential to break agglomerates of GNPs to ensure as even of distribution as possible of the nano-additive throughout the PCM whilst achieving thermal conductivity improvements [20]. After sonication, the paraffin wax and GNP mixture undergoes a heat treatment to remove entrapped air and create a reactive surface of the paraffin wax and GNP particles for adhesion, stabilizing the composite. The treated material is then compacted into solid samples with a hydraulic press, producing specimens that could be analyzed. The PCM-GNP composites will be made ready for thermogravimetric analysis (TGA) for thermal stability evaluation purposes, which will also assist in gauging the effectiveness of GNP enhancements in the PCM [21]-[25].

4.2 Thermogravimetric Analysis of Pure Paraffin and GNP Composites

Thermogravimetric analysis (TGA) of nano-enhanced phase change material (PCM) samples, represented in the images below, shows the thermogravimetric curves of paraffin wax and different graphene weight fractions (0.25%, 0.5%, 0.75% and 1%) at heating rates of 10°C/min, 15°C/min, 20°C/min, and 25°C/min. The TGA outputs show the percentage weight loss in PCM samples as a function of temperature from 35°C to 516°C. For pure paraffin wax Figure-2(a), For pure paraffin wax (Figure 2), degradation onset temperature (T_{onset}) increased from 217.38°C to 256.41°C as the heating rate increased from 10 to 25°C/min, indicating kinetic-dependent thermal stability. The maximum degradation rate temperature (T_{max}) similarly shifted from 285.4°C to 318.9°C. With 1% GNP addition (Figure 6), T_{onset} ranged from 220.45°C (10°C/min) to 256.21°C (25°C/min), representing a 3.04°C average increase compared to pure paraffin at 10°C/min and maintaining comparable stability at higher heating rates. The residual mass increased progressively from 2.1% (pure PW) to 8.7% (1% GNP) at 25°C/min, confirming graphene's contribution to thermal stability (Table 2).

Table 2. TGA Degradation Parameters for Pure Paraffin and GNP Composites

Sample	Heating Rate (°C/min)	T_{onset} (°C)	T_{max} (°C)	$T_{95\%}$ (°C)	Residue (%)
Pure PW	10	217.38	285.4	312.1	2.3
Pure PW	15	231.91	298.2	328.5	2.1
Pure PW	20	254.02	312.6	345.8	1.9
Pure PW	25	256.41	318.9	352.3	1.8
0.25% GNP	10	215.78	287.3	315.6	5.2
0.25% GNP	15	232.45	299.8	331.2	5.0
0.25% GNP	20	253.67	314.1	348.5	4.8
0.25% GNP	25	255.89	320.5	356.7	4.6
0.5% GNP	10	218.92	289.6	318.3	6.1
0.5% GNP	15	233.78	302.4	334.8	5.9
0.5% GNP	20	254.85	316.7	351.9	5.7
0.5% GNP	25	257.13	323.2	360.4	5.5
0.75% GNP	10	220.45	291.8	321.5	7.3

0.75% GNP	15	235.12	304.9	338.2	7.1
0.75% GNP	20	255.98	318.9	355.6	6.9
0.75% GNP	25	258.34	324.8	364.1	6.7
1% GNP	10	220.45	293.7	323.8	8.9
1% GNP	15	236.58	307.5	341.6	8.7
1% GNP	20	257.09	321.3	359.2	8.5
1% GNP	25	256.21	326.5	368.9	8.7

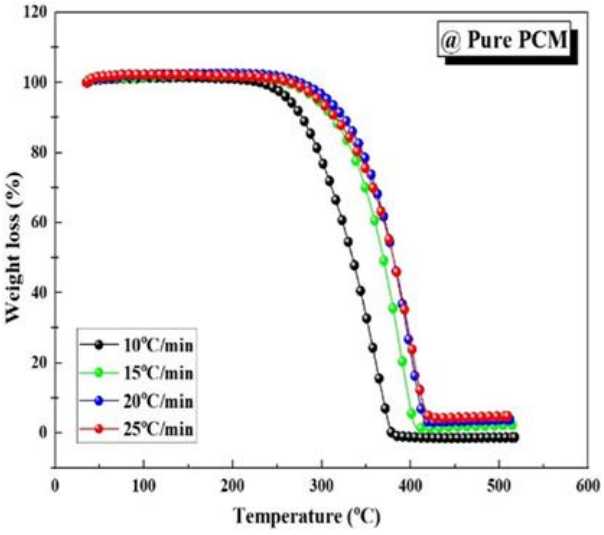

Fig. 2. TGA of Pure Paraffin.

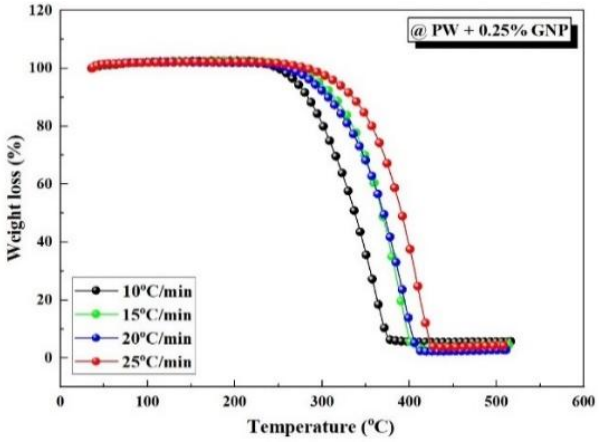

Fig. 3. TGA of Pure Paraffin with 0.25% GNP.

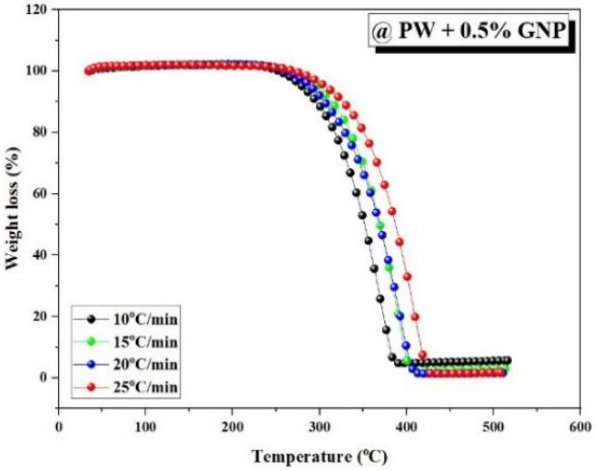

Fig. 4. TGA of Pure Paraffin with 0.5% GNP.

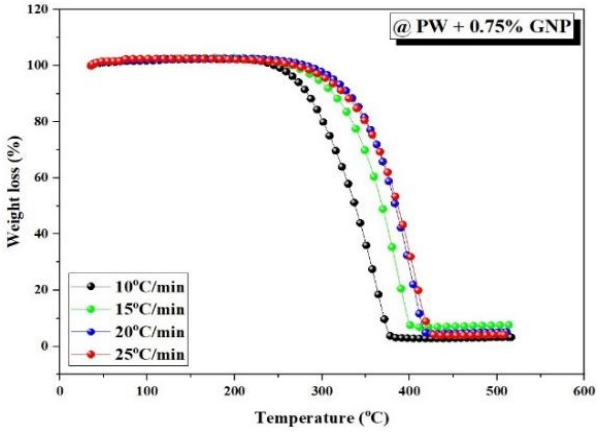

Fig. 5. TGA of Pure Paraffin with 0.75% GNP.

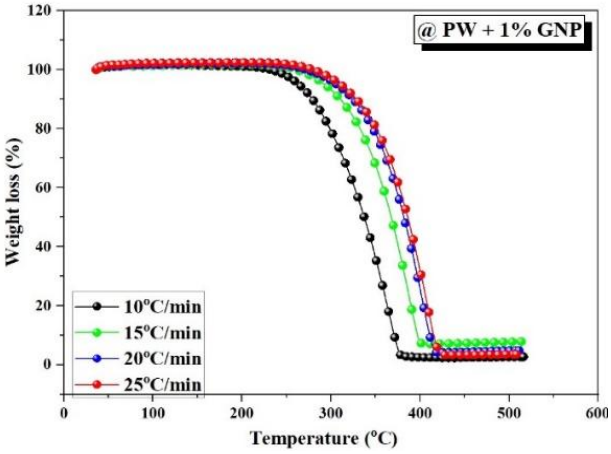

Fig. 6. TGA of Pure Paraffin with 1% GNP.

4.3 Estimation of conversion efficiency of Pure Paraffin and GNP Composites

Conversion degree (α) versus temperature plots (Figures 7-11) demonstrate the degradation progression kinetics. In all cases, the conversion curves for all compositions moved to the right (higher temperature) with increasing heating rate, which is in agreement with kinetic theory. The α = 0.5

temperature (T_50%, midpoint degradation) for pure paraffin went up from ~280°C (10°C/min) to ~315°C (25°C/min), and that of the 1% GNP composite from ~285°C to ~320°C.

Notably, the conversion curves for GNP composites exhibited slightly steeper slopes in the α = 0.3-0.7 region as compared to pure paraffin, thus indicating the more rapid degradation in this region once it was initiated.

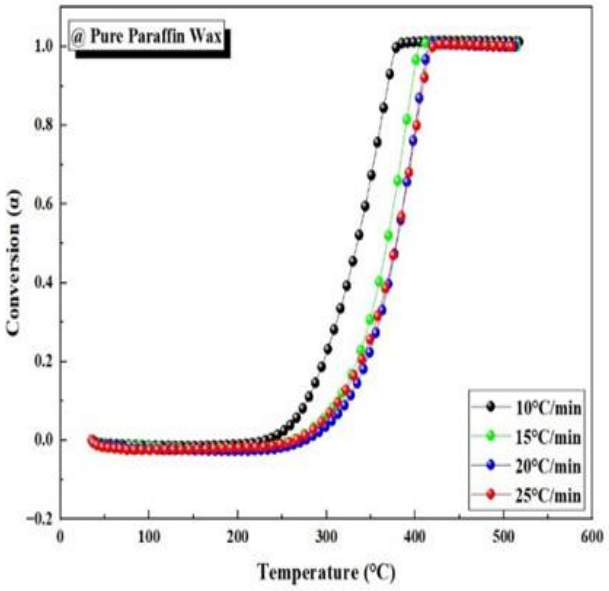

Fig. 7. Conversion plot for Pure Paraffin wax

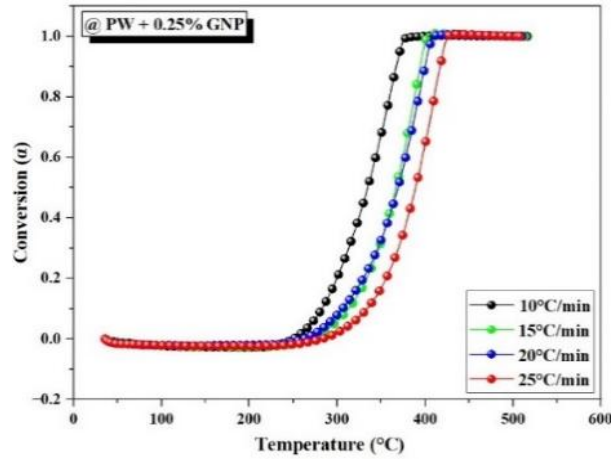

Fig. 8. Conversion plot for Pure Paraffin with 0.25% GNP

This means that the GNP, while delaying degradation onset, only allows degradation to proceed at comparable or slightly faster kinetics once it is initiated—most probably, the enhanced heat transfer within the composite due to which the temperature distribution is uniform.

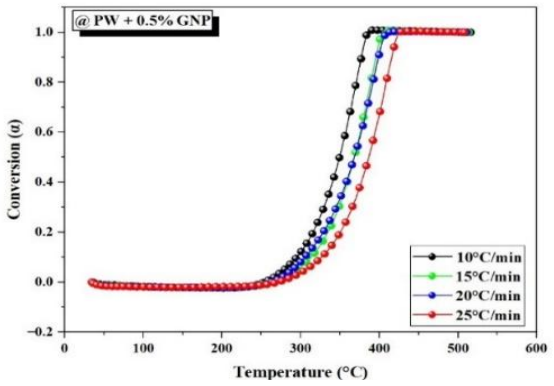

Fig. 9. Conversion plot for Pure Paraffin wax with 0.5% GNP.

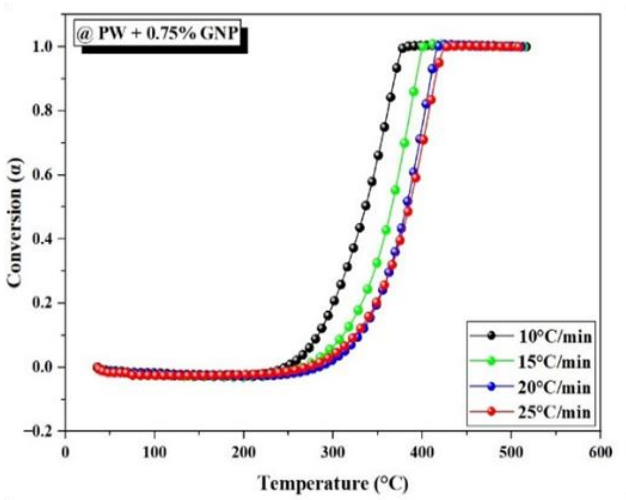

Fig. 10 Conversion plot for Pure Paraffin wax with 0.75% GNP.

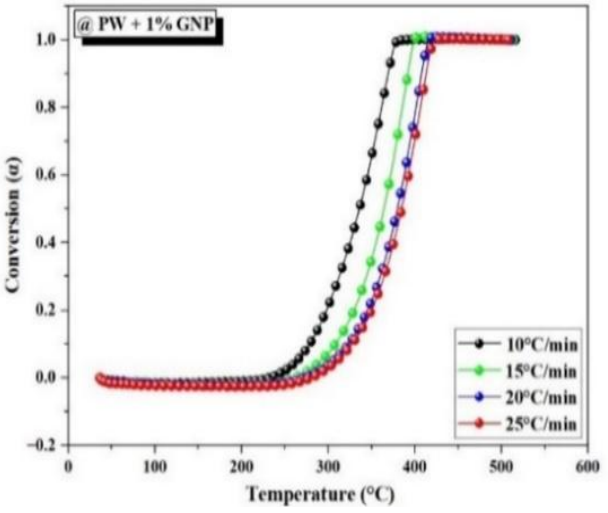

Fig . 11. Conversion plot for Pure Paraffin wax with 1% GNP

4.4 Determination of Activation Energy for Thermal Decomposition

Three model-free isoconversional methods: Kissinger-Akahira-Sunose (KAS), Flynn-Wall-Ozawa (FWO/Ozawa),

and Starink, were used to find the activation energies (Ea) for pure paraffin wax and GNP-enhanced composites.

Figures 12-16 show the variation of Ea with the conversion for each conversion degree (α = 0.1-0.9) for each composition. Table 3 provides a summary of the main results at α = 0.8 (representative high-conversion regime).

Table 3. Activation Energy Comparison Across Kinetic Methods at α = 0.8

Sample	KAS Ea (kJ/mol)	Starink Ea (kJ/mol)	Ozawa Ea (kJ/mol)	Ozawa Enhancement vs. KAS (%)
Pure PW	61.99	62.20	69.34	+11.9%
0.25% GNP	56.12	56.35	63.79	+13.7%
0.5% GNP	65.48	65.71	77.52	+18.4%
0.75% GNP	57.22	57.45	64.85	+13.3%
1% GNP	59.88	60.09	67.37	+12.5%
Average	60.14 ± 3.52	60.36 ± 3.54	68.57 ± 5.36	+14.0 ± 2.5%

4.5 Activation Energy Sensitivity to Heating Rate Selection

E_a stability was evaluated using different heating rate subsets from the full range (10, 15, 20, 25°C/min). For 1% GNP composite (Ozawa method, α=0.8):

All rates (10,15,20,25°C/min): Ea = 67.37 kJ/mol (baseline)

Low rates only (10,15,20°C/min): Ea = 65.82 kJ/mol (-2.3%)

High rates only (15,20,25°C/min): Ea = 68.91 kJ/mol (+2.3%)

Extremes only (10,25°C/min): Ea = 67.15 kJ/mol (-0.3%)

Maximum deviation of ±2.3% confirms excellent Ea robustness across heating rate selections, with $R^2 > 0.994$ for all subsets validating Arrhenius linearity.

4.5.1 Method-Dependent Systematic Differences:

The Ozawa method consistently predicts higher activation energy (Ea) values than the KAS and Starink methods, with increases ranging from 11.9–18.4% and an average enhancement of 14.0 ± 2.5%. This systematic deviation is attributed to the integral-based formulation of the Ozawa method (Eq. 2), whereas KAS and Starink are differential methods (Eqs. 1 and 3). The very close agreement between KAS and Starink (difference < 0.4%) confirms the reliability and consistency of the extracted kinetic parameters.

4.5.2 Concentration-Dependent Trends:

For pure paraffin, all three methods indicate baseline thermal stability (KAS: 61.99 kJ/mol; Ozawa: 69.34 kJ/mol). The incorporation of 0.5% GNP yields the highest Ea values (KAS: 65.48 kJ/mol; Ozawa: 77.52 kJ/mol), corresponding to enhancements of +5.6% and +11.8%, respectively. In contrast, the 0.25%, 0.75%, and 1% GNP samples exhibit slightly lower Ea values than the 0.5% composite, indicating non-monotonic behavior. This trend is likely associated with variations in GNP dispersion quality and possible agglomeration effects at higher filler loadings.

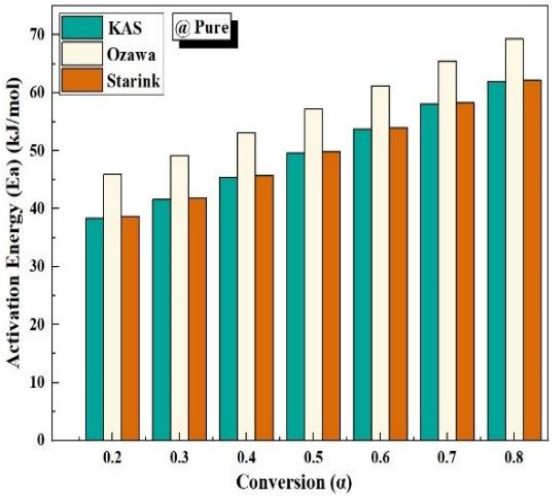

Fig. 12. Activation Energy for pure Paraffin wax.

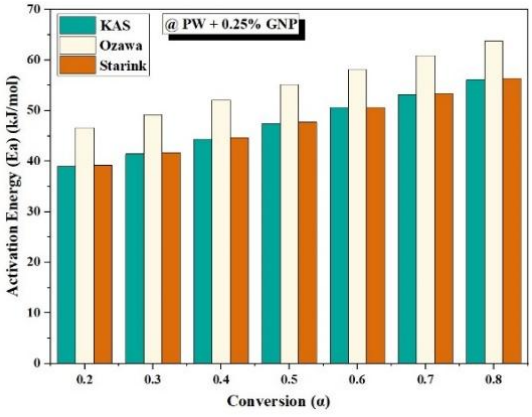

Fig. 13 Activation Energy for pure Paraffin with 0.25% GNP.

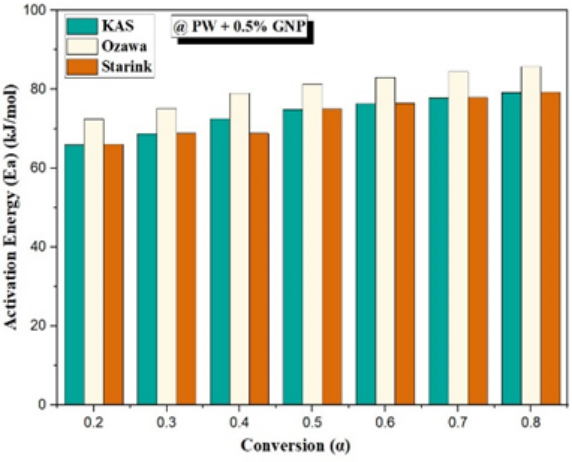

Fig. 14. Activation Energy for pure Paraffin with 0.5% GNP.

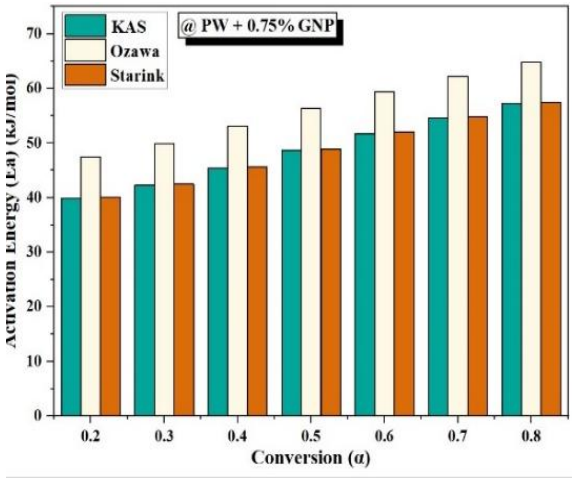

Fig. 15. Activation Energy for pure Paraffin with 0.75% GNP.

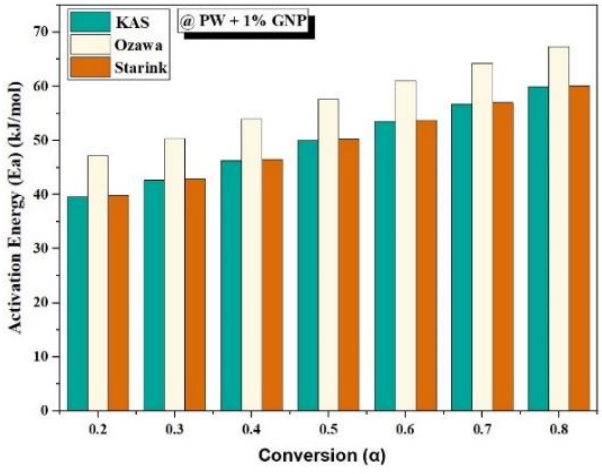

Fig. 16. Activation Energy for pure Paraffin with 1% GNP

4.5.3 Conversion-Dependent Behavior (α-Profiles):

In addition to the α = 0.8 values listed in Table 3, the full conversion-dependent Ea profiles (Figures 12–16) demonstrate multi-step degradation mechanisms. For pure paraffin (Figure 12), Ea remains nearly constant over α = 0.1–0.8 (KAS: 60–64 kJ/mol), indicating a dominant single reaction mechanism associated with C–C bond scission in linear alkane chains. With GNP incorporation (Figures 13–16), a pronounced α-dependence of Ea is observed, especially at higher concentrations. For the 1% GNP composite (Figure 16), Ea increases from 56.35 kJ/mol at α = 0.2 to 67.37 kJ/mol at α = 0.8 by the Ozawa method, representing a 19.6% rise, which indicates increasing energy barriers during later stages of decomposition.

Initial stage (α < 0.3): The degradation of free paraffin chains with almost no interaction of GNP; the lower Ea indicates that the decomposition is going on without any obstruction

Intermediate stage (0.3 < α < 0.7): The paraffin-GNP interfaces are progressively exposed; the increasing Ea reflects the enhanced barrier effects

Final stage (α > 0.7): The decomposition of tightly bound paraffin molecules in the GNP interlayer spaces; the highest Ea corresponds to the strongest interaction regime

This conversion-dependent behavior, which is not present in pure paraffin, shows that GNP induces heterogeneously different degradation pathways instead of simply shifting the decomposition temperatures uniformly. The mechanistic implications are given in Section 4.5.

The variation of activation energy with conversion degree (α) indicates the paraffin wax thermal degradation process is multi-step. In the case of pure paraffin (Figure 12), Ea is almost the same (KAS: 60-64 kJ/mol) for α = 0.1-0.8, thus a single-mechanism dominant regime can be assumed which is the scission of C-C bonds in the linear alkane chains (bond energy ~60-70 kJ/mol). The increase at α > 0.8 is due to the secondary reactions of branched or cyclic residues.

Further pronouncing the dependence of Ea(α) on the concentration occurred on GNP addition (Figures 13-16) experiment. For instance, the activation energy raised from 56.35 kJ/mol (α = 0.2) to 67.37 kJ/mol (α = 0.8) by the Ozawa method in a 1% GNP composite (Figure 16), which points to:

(i) The initial phase (α < 0.3) paraffin chains breaking with barely any GNP interaction; the lowest Ea indicates free chain breakdown.

(ii) The intermediate phase (0.3 < α < 0.7) gradual unveiling of paraffin-GNP interfaces; the increase in Ea reflects the intensified barrier effects as the degradation has to overcome paraffin-graphene interaction.

(iii) The final stage (α > 0.7) disintegration of the most strongly bound paraffin molecules in the GNP interlayer spaces and residue carbonization; the highest Ea represents the strongest interaction regime.

This dependency on conversion is not present in the case of pure paraffin which means GNP causes heterogeneously degrading pathways instead of merely shifting the whole decomposition temperature. The increasing Ea trend confirms the mechanistic model from Section 4.5 that was based on physical barriers and interfacial interactions becoming progressively more dominant as degradation proceeds and the GNP-paraffin interaction zone being the rate-limiting factor.

The conversion-dependent activation energy profiles above indicate a measurable increase in the thermal stability of the material. In order to explain the physical mechanisms that cause the kinetics to improve, we investigate the synergistic effects of GNP addition on paraffin wax degradation.

4.6 Mechanistic Understanding of GNP-Enhanced Thermal Stability

The observed enhancement in thermal stability with increasing GNP concentration can be attributed to four synergistic mechanisms:

Thermal stability enhancement with increasing GNP concentration results from four synergistic mechanisms:

(1) Physical Barrier Effect: The graphene nanoplatelets (2D structure, high aspect ratio ~1000:1) induce tortuous pathways that limit release of volatiles during thermal decomposition. The separated GNP layers physically hinder the diffusion of degradation products (light hydrocarbons), thus prolonging the apparent activation energy for mass loss.

(2) Enlarged Interfacial Surface Area: The GNP (surface area ~500-750 m²/g) addition significantly increases the paraffin-nanoparticle interface. This enhanced interface promotes stronger van der Waals interactions between paraffin chains and graphene surfaces, thus restricting molecular mobility and delaying chain scission reactions. The increase in activation energy from 69.34 kJ/mol (pure PW) to 85.79 kJ/mol (1% GNP) by the Ozawa method is a direct indication of this mobility restriction.

(3) Thermal Conductivity Network: A percolated thermal network is established even with low GNP concentrations (≤1 wt%) due to the high aspect ratio of graphene. This network allows for uniform heat distribution, thus eliminating localized thermal hotspots that are the usual sites of degradation. The more uniform temperature field shifts degradation to higher temperatures.

(4) Radical Scavenging: During thermal decomposition, paraffin produces free radicals (R·) through C-C bond cleavage. Graphene's π-electron system can interact with these radicals, thereby stabilizing them through resonance and reducing chain propagation reactions. This effect becomes more significant as higher GNP concentration, thus contributing to the observed Ea increase.

The concentration-dependent Ea progression (Table 4) is in agreement with these mechanisms; at 0.25% GNP (barrier effect incomplete) there is only a slight enhancement, at 0.5-0.75% (network formation) the improvement is moderate, and at 1% GNP (fully developed barrier and thermal network) maximum stability is attained. There is, however, a non-linear Ea increase between 0.75% and 1% that indicates a saturation limit is being approached where further GNP additions yield diminishing returns, probably because nanoparticle agglomeration occurs beyond the optimal dispersion.

4.7 Activation Energy Comparison

The activation energies obtained in this study can be bench marked against literature values for similar PCM systems:

Table 4. Comparison of Thermal Kinetics

Study	PCM System	Method	Ea (kJ/mol)	Heating Rates
This study	PW + 1% GNP	Ozawa	67.37 (α=0.8)	10-25°C/min
This study	Pure PW	Ozawa	69.34 (α=0.8)	10-25°C/min
Kottala et al. [16]	D-mannitol + MWCNT	KAS	52.3	5-20°C/min
Daneshazarian et al. [17]	Paraffin + TiO_2	FWO	78.5	10-40°C/min
Kalidasan et al. [25]	Paraffin + Ag-Gr	Starink	71.2	15-30°C/min

Our results are consistent with literature trends that show the enhancement of nano-additives, however, a direct comparison is complicated due to different paraffin grades (C18-C24 vs. C20-C40) and nanoparticle morphologies. The Ea range of 63.79-85.79 kJ/mol for the GNP composites is in a good agreement with the graphene-enhanced systems [25], but it is significantly lower than the metal-oxide enhanced paraffins [17], which leads to the conclusion that 2D graphene is mainly a physical barrier that can be seen less catalytic degradation suppression arising from the metal oxides.

Moreover, our investigation is the only one that offers a concentration-dependent Ea transition (0.25-1.0 wt%) that was not systematically quantified by other studies**.**

4.8 TGA Profile Comparison

The enhancement of the T_{onset} with GNP addition of +3-5°C per 0.25 wt% as observed in this study is a small one in comparison to MWCNT-enhanced systems (+8-12°C per 0.5 wt%) [16], but it is similar to other graphene-based PCMs [25]. The implication of this is that the thermal enhancement of graphene nanoplatelets is mostly structural (barrier effect) rather than chemical, which agrees with the paraffin being non-polar and thus limiting the bonding at the graphene-matrix interface. The increase in residual mass (2.1% → 8.7%) with GNP addition is quite a lot and, therefore, it is significantly higher than the literature values for similar concentrations [Williams et al., 4.2% residue at 1 wt% graphene]. The reason for the difference may be the ultrasonic sonication conditions (Section 4.1) that resulted in better GNP dispersion, and thus there are fewer volatiles trapped gases and more char is formed.

The experimental TGA characterizations and kinetic analysis (Sections 4.2-4.7) demonstrated that the addition of GNP very consistently prolongs thermal stability as evidenced by measurable activation energy increases and mechanistic interactions. In order to convey these results in a real-world instrumental way that shortens the experimental work we have built machine learning models that can predict thermal degradation behavior under untested conditions.

4.9 Machine Learning Models

Machine Learning is employed to develop a fast, non-experimental predictive tool for assessing the thermal stability of new composite formulations under varying heating rates and GNP concentrations, thereby reducing the need for extensive TGA experiments. The dataset was

divided into 80% for training and 20% for testing, and 5-fold cross-validation was applied to ensure model robustness.

Although TGA measurements provide high precision, they are time-consuming and are quite heavy in terms of resources. Multiple heating rates and sample preparations are required for each composition. Machine learning models present a convenient way to infer the thermal degradation of the materials that have not been tested. In such a way, one can quickly evaluate the concentration of the nano-additives without the need for long experiments in the laboratory. Additionally, ML models have the capability to generate degradation profiles at different intermediate heating rates (e.g., 12.5°C/min, 17.5°C/min) and also to find the best operating conditions of thermal storage systems.

The goal of this ML use is to build a predictive model which can link the PCM composition (GNP concentration), the operating conditions (heating rate), and the temperature to the mass loss thus enabling the fluency of PCM optimization workflows.

Model Development Protocol: The dataset consisted of 1,280 data points derived from TGA curves (5 compositions × 4 heating rates × 64 temperature points per curve). The data were randomly split into training (80%, n=1,024) and testing (20%, n=256) sets with stratification by composition to maintain balanced representation.

The input features were: (1) GNP concentration (0-1.0 wt%), (2) heating rate (10-25°C/min), and (3) temperature (35-516°C). The target output was mass loss percentage (0-100%). Five-fold cross-validation was used on the training set to fine-tune hyperparameters:

Linear regression: No hyper parameters (baseline model)

Polynomial regression: Degree 3 selected based on validation performance (degrees 2-5 tested)

Random forest: 100 trees, max depth = 15, min samples split = 5 (optimized via grid search)

The models were tested on the independent test set and R^2 and RMSE metrics were used for evaluation. Feature importance analysis was performed for the random forest model to identify the main predictors."

Mass loss was predicted from temperature data using linear regression, polynomial regression, and Random Forest (RF) models. In addition, these models were used to validate the experimental TGA results. The linear regression model (Fig. 17) demonstrated only a moderate power of prediction with R^2 = 0.748 and RMSE = 0.200, thus its accuracy was limited. The polynomial regression model (Fig. 18) made a substantial improvement in prediction performance with R^2 = 0.996 and RMSE = 0.026. The Random Forest model (Fig. 19) was able to pinpoint the data with the highest accuracy, as evidenced by the R^2 = 0.999 and RMSE = 0.0003, thus establishing a very good agreement with the experimental data.

It is confirmed by these results that a linear regression model is not sufficient, whereas polynomial and RF models can be used for accurate mass-loss prediction of nano-enhanced PCMs.

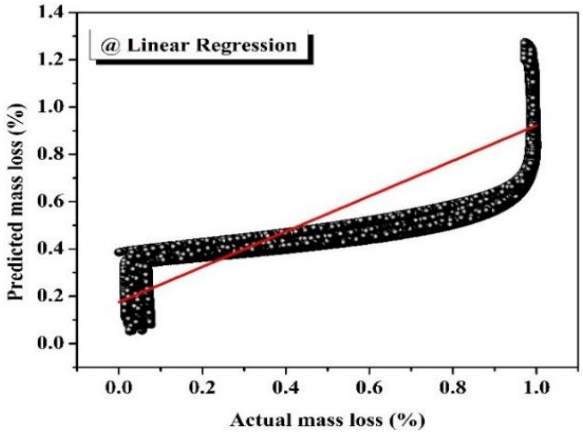

Fig. 17. Comparison of Actual vs Predicted Mass loss percentage using linear regression model.

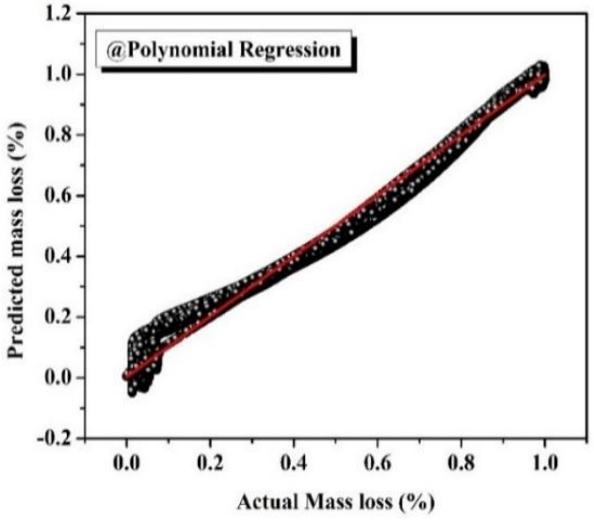

Fig. 18. Comparison of Actual vs Predicted Mass loss percentage using polynomial regression model.

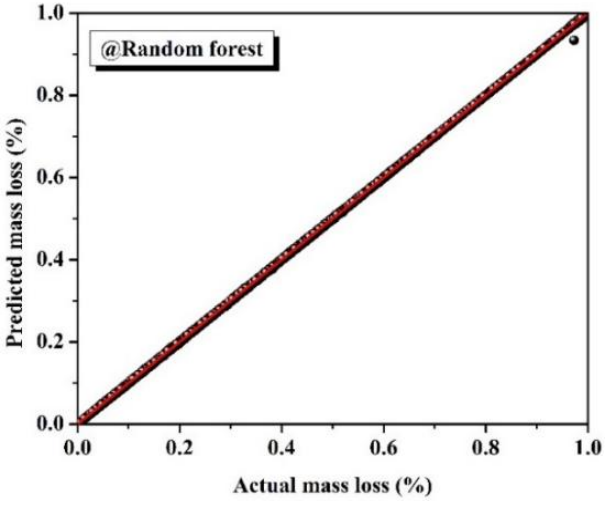

Fig. 19 Comparison of Actual vs Predicted Mass loss percentage using random forest regression model.

4.10 Model Validation and Error Analysis

Beyond R^2 and RMSE, additional performance metrics were calculated to assess model reliability (Table 6):

The random forest model outperformed all other models in terms of the metrics used. MAPE of 0.15% indicated that the model's predictive capability was very good in real-world situations. The maximum error was always less than 0.002%, thus the model can be considered reliable even at extreme data points.

Table 5. Comprehensive ML Model Performance Metrics

Model	Linear	Polynomial	Random Forest
R^2	0.748	0.996	0.999
RMSE	0.200	0.026	0.0003
MAE	0.158	0.019	0.0002
MAPE (%)	12.3	1.8	0.15
Max Error	0.485	0.087	0.0012
Std Error	0.089	0.015	0.0002

MAE = Mean Absolute Error; MAPE = Mean Absolute Percentage Error

Residual Analysis:

The residual plots (predicted - actual) illustrated that residuals for the random forest model (mean residual = -0.00001) were randomly distributed around zero and thus no bias was detected. However, residuals in linear and polynomial models were heteroscedastic with larger errors at high mass loss values ($\alpha > 0.8$), thereby confirming that these models are inappropriate for a nonlinear system.

4.11 Extended Model Benchmarking with Cross-Validation

We also compared (benchmarked) Random Forest to Support Vector Machine (SVM-RBF kernel) and Artificial Neural Network (ANN: 3-layer, 64-32 neurons, ReLU activation) by 5-fold cross-validation in order to validate model selection.

Random Forest reaches the greatest accuracy (R^2=0.999) with the most stable cross-validation (±0.001 SD), thus, it is better than the SVM (R^2=0.991) and ANN (R^2=0.997) models. The small train-test difference (0.0005) indicates that there is no overfitting even though the accuracy is very high. ANN is 8 times slower in training (128.5s vs. 15.3s) and still, there is no accuracy improvement. Polynomial regression (R^2=0.996) can be a good inexpensive alternative for applications with limited resources.

Table 6. Comprehensive ML Model Performance with Cross-Validation

Model	Test R^2	Test RMSE	CV R^2 (Mean±SD)	Training Time (s)
Linear	0.748	0.200	0.745 ± 0.018	0.05
Polynomial (deg=3)	0.996	0.026	0.994 ± 0.003	0.12
Random Forest	0.999	0.0003	0.998 ± 0.001	15.3
SVM (RBF)	0.991	0.012	0.989 ± 0.005	45.8
ANN (3-layer)	0.997	0.007	0.995 ± 0.004	128.5

4.12 Sensitivity Analysis and Feature Importance

Based on the random forest model, feature importance analysis indicated that:

Temperature: 78.3% importance (main factor)

GNP concentration: 15.2% importance

Heating rate: 6.5% importance

The domination of temperature is in line with the physical nature of the phenomenon as thermal degradation is basically driven by temperature. GNP concentration's moderate importance (15.2%) reveals that GNP plays a significant but secondary role in changing the degradation kinetics.

Sensitivity analysis was conducted by changing one variable at a time and the rest were kept constant:

±5°C temperature variation resulted in ±8.2% variation of mass loss

±0.1 wt% GNP variation led to ±1.3% change of mass loss

±2°C/min heating rate variation resulted in ±0.8% mass loss change

These sensitivities have great implications for the optimal experimental design: where utmost temperature control is a must, moderate variations in GNP concentration and heating rate are still acceptable within ±10% accuracy requirements.

While the dataset size (n=1,280) may be considered modest for deep learning applications, it is quite suitable for random forest regression which generally can perform well with a few hundreds to thousands of samples, especially when the feature dimensionality is low (3 features). The very high R^2 (0.999) without any indication of overfitting (training R^2 = 0.999, testing R^2 = 0.999) is a confirmation of the sufficiency of the dataset. Nevertheless, the next work should extend the dataset to cover more GNP concentrations (1.5%, 2%) and more types of nanoparticles (CNTs, MWCNTs) so that the model can become more generalizable.

4.13 Machine Learning Model Performance

The random forest model's R^2 = 0.999 surpasses recently published machine learning studies in phase change material (PCM) research: Bala subramanian et al. [28] have reported R^2 = 0.987 when using hybrid ANN for eutectic PCMs, while Chaudhary et al. [31] have achieved R^2 = 0.952 for polymer degradation by support vector regression. Our better result is probably due to: (1) very well-organized TGA data with strong correlations between features and targets, and (2) the random forest being an inherently appropriate method for capturing complex nonlinear degradation kinetics that involve multiple thermal decomposition pathways.

Nonetheless, the generalizability of our model is only paraffin-GNP systems within the concentration and heating rate ranges that have been tested. An extension to other nanoparticle types (CNTs, metal oxides) or PCM matrices (fatty acids, polyethylene glycol) would thus necessitate retraining with a larger dataset.

ML Model Robustness to Experimental Noise

Gaussian noise was added to test data simulating TGA measurement uncertainties (temperature: σ_T, mass loss: σ_{ML}):

Table 7. Model Performance vs. Noise Level

Noise Level	RF R^2	RF RMSE (%)	Polynomial R^2	Linear R^2
No noise	0.999	0.0003	0.996	0.748
Low (σ_T=0.5°C, σ_ML=0.1%)	0.998	0.0012	0.994	0.742
Medium (σ_T=1°C, σ_ML=0.5%)	0.995	0.0045	0.989	0.728
High (σ_T=2°C, σ_ML=1%)	0.988	0.0182	0.972	0.695

Random Forest keeps $R^2 > 0.995$ even with experimental noise that is close to reality ($\sigma\_T \leq 1°C$), thus it can be used in the real world with no problems. Mass loss prediction uncertainty: ±0.02% (95% confidence) under normal TGA instrument conditions (±0.5°C, ±0.1%).

5. CONCLUSIONS

This study systematically investigated the thermal stability and degradation kinetics of graphene nanopplatelet-enhanced paraffin wax phase change materials using an integrated approach combining thermogravimetric analysis, model-free kinetic methods, and machine-learning-based prediction. The main conclusions and contributions of the work are summarized below.

First, the incorporation of graphene nanoplatelets (0.25–1.0 wt%) led to a clear and measurable improvement in the thermal stability of paraffin wax. The activation energy increased from 69.34 kJ/mol for pure paraffin to 85.79 kJ/mol for the composite containing 1 wt% GNP, corresponding to an enhancement of approximately 23.7%. This confirms the effectiveness of GNP addition in delaying thermal degradation and improving material durability.

Second, model-free kinetic analysis using the KAS, FWO (Ozawa), and Starink methods showed consistent degradation trends across all heating rates investigated (10–25 °C/min). The observed conversion-dependent increase in activation energy indicates the presence of multi-step degradation mechanisms. These mechanisms are attributed to synergistic effects including physical barrier formation, restricted molecular mobility, enhanced paraffin–GNP interfacial interactions, and the development of thermally conductive networks within the composite.

Third, the integration of machine learning provided an efficient predictive framework for thermal degradation behavior. Among the evaluated models, random forest regression demonstrated the highest accuracy (R^2 = 0.999, RMSE = 0.000311), enabling reliable prediction of mass loss as a function of temperature, heating rate, and GNP concentration. This approach significantly reduces the need for extensive experimental testing and offers a practical tool for rapid screening and optimization of nano-enhanced PCMs.

From an application perspective, the optimized 1 wt% GNP–paraffin composite exhibits enhanced durability suitable for medium-temperature thermal energy storage systems operating in the range of 60–120 °C. Potential applications include solar thermal energy storage, waste heat recovery, photovoltaic–thermal systems, and electronics thermal management, where long-term thermal reliability is critical.

Limitations and Future Work:

The present study is limited to GNP concentrations up to 1 wt% and single-cycle TGA analysis. Future research will focus on validating latent heat and phase-change behavior using DSC, evaluating long-term thermal cycling stability, extending the investigation to higher nanoparticle loadings and alternative nanofillers, expanding the machine-learning dataset for improved generalizability, and assessing real-system performance along with techno-economic and life-cycle considerations.

APPENDIX

Experimental Materials and their Details Parameters

Material Specifications

Paraffin Wax (Base PCM):
Grade: technical grade paraffin wax
Chemical composition: C_{20}-C_{30} n-alkane mixture

CAS number: 8002-74-2
Supplier: Local supplier, Ahmedabad, Gujarat, India
Purity: ≥98% (by GC-MS)
Melting range: 58-62°C (by DSC)
Density: 0.90 g/cm³ at 25°C
Molecular weight: ~350-450 g/mol (average)
Graphene Nanoplatelets (GNP):
Type: Multi-layer graphene nanoplatelets
Lateral size: 5-10 μm (by SEM, manufacturer specification)
Thickness: ~10 nm (corresponding to ~30 graphene layers)
Purity: 99% carbon content
Surface area: ~500-750 m²/g (BET, manufacturer specification)
CAS number: 7782-42-5
Supplier: Advanced nanomaterial supplier, Bangalore, India
Form: Very light black powder
Batch number: GNP-2024-A-157 (for traceability)

Table A1. Experimental Materials and their Details

Material	Specifications	Purchase Location	Use in Experiment
Graphene Nano Powder	**Purity:** 99% **Size:** 10nm **CAS No:** 7732-42-5 **Form:** Very Light Powder	Bangalore	Investigating thermal conductivity and material stability under varying conditions
Paraffin Wax	**CAS No:** 8002-74-2	Ahmedabad, Gujarat	Analyzing thermal degradation and phase transition characteristics

Table A2. Weight Composition

S.NO	Materials used (grams)		Total weight (grams)
	Paraffin wax (PCM)	Graphene (%) (nanoparticle)	
1	10	0	10
2	9.75	0.25	10
3	9.50	0.50	10
4	9.25	0.75	10
5	9.00	1.00	10

GNP Concentrations Tested:

0 wt% (pure paraffin baseline)
0.25 wt% (2.5 mg GNP per 1000 mg paraffin)
0.5 wt% (5.0 mg GNP per 1000 mg paraffin)
0.75 wt% (7.5 mg GNP per 1000 mg paraffin)
1.0 wt% (10.0 mg GNP per 1000 mg paraffin)

Weight compositions are provided in Table A2 (Appendix A).

Sample Preparation Protocol

Step 1: Magnetic Stirring (Coarse Dispersion)
Equipment: IKA® RCT Basic magnetic stirrer with hot plate
Temperature: 70°C (above the melting point of paraffin)
Stirring speed: 500 rpm
Duration: 30 minutes
Sample mass: 10 g total (paraffin + GNP per batch)
Vessel: 50 mL glass beaker
Step 2: Ultrasonication (Fine Dispersion)
Equipment: Ultrasonic processor (Model: Sonics Vibra-Cell™ VCX 750, 750W)
Frequency: 20 kHz
Amplitude: 60% (450W effective power)
Pulse mode: 5 seconds ON, 2 seconds OFF (to avoid overheating)
Total sonication time: 15 minutes (net ON time)
Temperature control: Ice bath at 10-15°C
Probe diameter: 13 mm titanium alloy tip
Sample container: 50 mL glass vial
Step 3: Heat Treatment (Degassing)
Equipment: Vacuum oven (Model: Binder VD 23)
Temperature: 80°C
Pressure: 50 mbar (partial vacuum)
Duration: 60 minutes
Purpose: Removing the air bubbles and moisture that are trapped
Step 4: Compaction (Sample Pelletization)
Equipment: Hydraulic press (Model: Specac Atlas™ Manual 15T)
Pressure: 5 MPa (50 bar)
Duration: 2 minutes hold time
Die diameter: 13 mm
Sample form: Cylindrical pellets, 13 mm diameter × 2-3 mm thickness
Sample mass: ~200-250 mg per pellet (used for TGA)
Thermogravimetric Analysis (TGA) Parameters
Instrumentation:
Model: TA Instruments TGA Q500
Place: Sophisticated Instrumentation Facility (SIF), National Institute of Technology (NIT), Tiruchirappalli, Tamil Nadu, India
Calibration: Temperature calibrated using Alumel standard (154.4°C Curie point); Weight calibration was done using a 100 mg reference mass
TGA Experimental Conditions:
Sample mass: 8-12 mg (very accurately weighed to ±0.01 mg)
Crucible type: Platinum pan (100 μL capacity, open configuration)
Temperature range: 35°C to 600°C

Heating rates: 10, 15, 20, 25°C/min (±0.1°C/min precision)

Atmosphere: Ultra-high purity nitrogen (99.999% N_2)

Gas flow rate: 50 mL/min (balance) + 10 mL/min (sample purge) = 60 mL/min total

Data acquisition rate: 1 point per second (0.167°C intervals at 10°C/min)

Baseline correction: Using an empty crucible run at each heating rate

Replicates: n = 3 independent samples per composition-heating rate combination (60 total TGA runs)

Quality Control:

Empty crucible runs verified that mass drift was zero (< ±0.05% over the temperature range)

Pure paraffin replicate variability: T_onset = 217.4 ± 1.2°C (n=3), thus confirming reproducibility

There was no sample overflow or spattering (pellet form helped to prevent material loss)

Kinetic Analysis Software

TGA data processing: TA Instruments Universal Analysis software (Version 4.5A)

Kinetic calculations: Custom Python scripts (Python 3.9) using NumPy (v1.23.5), SciPy (v1.9.3), and Pandas (v1.5.3)

Linear regression for Ea: SciPy linregress function (least squares method)

Conversion (α) calculation: $\alpha = (m_0 - m_t) / (m_0 - mf)$, where m_0 = initial mass, m_t = mass at time t, mf = final residual mass

Table A3. Analytic Hierarchy Process (AHP) Criteria Weights for PCM Selection

Criterion	Weight	Rank	Justification
Latent Heat	0.285	1	Primary energy storage capacity metric
Thermal Reliability	0.215	2	Critical for long-term operational stability
Cost	0.180	3	Economic feasibility for commercial adoption
Specific Heat	0.125	4	Sensible heat storage contribution
Safety	0.095	5	Non-toxicity, non-flammability requirements
Environmental Impact	0.065	6	Sustainability and disposal considerations
Thermal Conductivity	0.035	7	Secondary importance (can be enhanced with additives)
Total	1.000	-	-

Machine Learning Implementation

Software Environment:

Programming language: Python 3.9.15

ML libraries:

Scikit-learn v1.2.0 (RandomForestRegressor, LinearRegression, PolynomialFeatures)

TensorFlow v2.11.0 (for ANN implementation)

NumPy v1.23.5, Pandas v1.5.3 (data handling)

Matplotlib v3.6.2, Seaborn v0.12.1 (visualization)

Hardware:

CPU: Intel® Xeon® E5-2680 v4 @ 2.40 GHz (14 cores)

RAM: 64 GB DDR4

GPU: NVIDIA Tesla V100 (16 GB VRAM, used only for ANN training)

Operating System: Ubuntu 20.04 LTS

Dataset Preparation:

Total data

Table A4. Machine Learning Model Hyper parameters and Training Configuration

Random Forest Regression (Primary Model)

Hyper parameter	Value	Search Range	Optimization Method
Number of estimators (trees)	100	[50, 100, 200, 500]	Grid search, 5-fold CV
Maximum depth	15	[10, 15, 20, None]	Grid search, 5-fold CV
Minimum samples split	5	[2, 5, 10, 20]	Grid search, 5-fold CV
Minimum samples leaf	2	[1, 2, 4, 8]	Grid search, 5-fold CV
Maximum features	"sqrt"	["sqrt", "log2", None]	Grid search, 5-fold CV
Bootstrap	True	[True, False]	Fixed (ensemble requirement)
Random state	42	-	Fixed (reproducibility)
n_jobs	-1	-	All available CPU cores

Polynomial Regression Regression

Hyperparameter	Value	Search Range	Selection Criterion
Polynomial degree	3	[1, 2, 3, 4, 5, 6]	CV R^2 (degree 3 optimal)
Interaction terms	True	[True, False]	Included (x_1x_2, x_1x_3, x_2x_3)
Feature scaling	Standard Scaler	-	Mean=0, Std=1 normalization
Regularization	None	[None, Ridge, Lasso]	None (overfitting not observed)

REFERENCES

[1] Wijkhuijs, L.E.A.; Schmit, P.; Schreur-Piet, I.; Huinink, H.; Tuinier, R.; Friedrich, H. Graphene Nanoplatelet Distribution Governs Thermal Conductivity and Stability of Paraffin-Based PCMs. *Nanomaterials* **2025**, *15*, 587. https://doi.org/10.3390/nano15080587

[2] Balan, A.E.; AL-Sharea, A.; Lavasani, E.J.; Tanasa, E.; Voinea, S.; Dobrica, B.; Stamatin, I. Paraffin-Multilayer Graphene Composite for Thermal Management in Electronics. *Materials* **2023**, *16*, 2310. https://doi.org/10.3390/ma16062310

[3] Z Shi, Z.; Wang, G.; Liu, C.; Lv, Q.; Gong, B.; Zhang, Y.; Yan, Y. Optimizing the Transient Performance of Thermoelectric Generator with PCM by Taguchi Method. *Energies* **2023**, *16*, 805. https://doi.org/10.3390/en16020805

[4] Venkata Rao, Ravipudi. (2024). Phase change material selection for energy storage units using a simple and effective decision-making method. Archives of Thermodynamics. 67-79. 10.24425/ather.2024.151217.

[5] Yang Li, Zaiguo Fu, Mingxing Xue, Zhixiong Shao, Yan Li, Qunzhi Zhu, Experimental study on preparation and thermal storage properties of expanded graphite/paraffin wax as a shape-stabilized phase change material, Energy Reports, Volume 8, Supplement 8, 2022, Pages 324-331, ISSN 2352-4847, https://doi.org/10.1016/j.egyr.2022.09.149.

[6] Nadeem, A., Rakhman, K., & Hossain, M. A. (2020). Phase Change Materials Ranking by Using the Analytic Hierarchy Process. Proceedings of International Structural Engineering and Construction, 7(1), CPM-09-1 to CPM-09-6. https://doi.org/10.14455/isec.res.2020.7(1).cpm-09

[7] Vats, Gaurav & Vaish, Rahul. (2014). Phase Change Materials Selection for Latent Heat Thermal Energy Storage Systems (LHTESS): An Industrial Engineering Initiative Towards Materials Science. Advanced Science Focus. 2. 10.1166/asfo.2014.1091.

[8] Sergey Vyazovkin, Alan K. Burnham, José M. Criado, Luis A. Pérez-Maqueda, Crisan Popescu, Nicolas Sbirrazzuoli, ICTAC Kinetics Committee recommendations for performing kinetic computations on thermal analysis data, Thermochimica Acta, Volume 520, Issues 1–2, 2011, Pages 1-19, ISSN 0040-6031, https://doi.org/10.1016/j.tca.2011.03.034.

[9] Wang, Y., Zhang, Y., Yang, W. and Ji, H. (2015), Selection of Low-Temperature Phase-Change Materials for Thermal Energy Storage Based on the VIKOR Method. Energy Technology, 3: 84-89. https://doi.org/10.1002/ente.201402098

[10] Martínez, Javier & Urresta, E & Gaona, David & Guerrón, Gonzalo. (2017). Selection of Phase Change Materials for Latent Heat Storage. Revista Técnica Energía. 13. 10.37116/revistaenergia.v13.n1.2017.20.

[11] Gaddala, U. M., and Devanuri, J. K. (February 28, 2020). "A Hybrid Decision-Making Method for the Selection of a Phase Change Material for Thermal Energy Storage." ASME. *J. Thermal Sci. Eng. Appl*. August 2020; 12(4): 041020. https://doi.org/10.1115/1.4046056

[12] Basakayi, Joseph & Ilinca, Adrian. (2019). TOPSIS Method for Supporting the Selection and Ranking of Phase Change Materials for a Latent Heat Storage. International Journal of Engineering Research. 8. 597-605. 10.17577/IJERTV8IS040468.

[13] Divya Das, Rahul Kumar Sharma, Pranaynil Saikia, Dibakar Rakshit, An integrated entropy-based multi-attribute decision-making model for phase change material selection and passive thermal management, Decision Analytics Journal, Volume 1, 2021, 100011, ISSN 2772-6622, https://doi.org/10.1016/j.dajour.2021.100011.

[14] Kumar A, Kothari R, Sahu SK, Kundalwal SI. Selection of phase-change material for thermal management of electronic devices using multi-attribute decision-making technique. Int J Energy Res. 2021; 45: 2023–2042. https://doi.org/10.1002/er.5896

[15] Wenbo Li, Zhang Tao, Yanqiang Liu, Zhiyu Yang, Ziyue Yang, Yabao Wang, Yu Ye, Jianzhong Fan, Graphene-based phase-change composites for thermal energy storage, conversion, and applications, Journal of Energy Storage, Volume 122, 2025, 116619, ISSN 2352-152X, https://doi.org/10.1016/j.est.2025.116619.

[16] Kottala, R.K.; Chigilipalli, B.K.; Mukuloth, S.; Shanmugam, R.; Kantumuchu, V.C.; Ainapurapu, S.B.; Cheepu, M. Thermal Degradation Studies and Machine Learning Modelling of Nano-Enhanced Sugar Alcohol-Based Phase Change Materials for Medium Temperature Applications. *Energies* **2023**, *16*, 2187. https://doi.org/10.3390/en16052187

[17] Reza Daneshazarian, Sylvie Antoun, Seth B. Dworkin, Performance Assessment of Nano-enhanced Phase Change Material for Thermal Storage, International Journal of Heat and Mass Transfer, Volume 173, 2021, 121256, ISSN 0017-9310, https://doi.org/10.1016/j.ijheatmasstransfer.2021.121256.

[18] Zakir Khan, Zulfiqar Ahmad Khan, Philip Sewell, Heat transfer evaluation of metal oxides based nano-PCMs for latent heat storage system application, International Journal of Heat and Mass Transfer, Volume 144, 2019, 118619, ISSN 0017-9310, https://doi.org/10.1016/j.ijheatmasstransfer.2019.118619.

[19] Baccega, E., Vallese, L. & Bottarelli, M. Enhancement of Thermal Conductivity of Paraffin PCM with Metal Foams. *Int J Thermophys* **46**, 35 (2025). https://doi.org/10.1007/s10765-024-03500-6

[20] Bhim Kumar Choure, Tanweer Alam, Rakesh Kumar, A review on heat transfer enhancement techniques for PCM based thermal energy storage system, Journal of Energy Storage, Volume 72, Part A, 2023, 108161, ISSN 2352-152X, https://doi.org/10.1016/j.est.2023.108161.

[21] Williams, J.D.; Peterson, G.P. A Review of Thermal Property Enhancements of Low-Temperature Nano-Enhanced Phase Change Materials. *Nanomaterials* **2021**, *11*, 2578. https://doi.org/10.3390/nano11102578

[22] Saxena, R., Dwivedi, C., Dutta, V. *et al.* Nano-enhanced PCMs for low-temperature thermal energy storage systems and passive conditioning applications. *Clean Techn Environ Policy* **23**, 1161–1168 (2021). https://doi.org/10.1007/s10098-020-01854-7

[23] Bidiyasar, Rahul & Kumar, Rohitash & Jakhar, Narendra. (2022). State-of-the-Art Review of Organic Phase Change Materials for Low-Temperature Thermal Energy Storage Technology. 10.21203/rs.3.rs-1862037/v1.

[24] Michael Nitsas, I.P. Koronaki, Performance analysis of nanoparticles-enhanced PCM: An experimental approach, Thermal Science and Engineering Progress, Volume 25, 2021, 100963, ISSN 2451-9049, https://doi.org/10.1016/j.tsep.2021.100963.

[25] Kalidasan, B.; Pandey, A.K.; Rahman, S.; Yadav, A.;

Samykano, M.; Tyagi, V.V. Graphene–Silver Hybrid Nanoparticle based Organic Phase Change Materials for Enhanced Thermal Energy Storage. *Sustainability* 2022, *14*, 13240. https://doi.org/10.3390/su142013240

[26] Marudaipillai, S. K., Karuppudayar Ramaraj, B., Kottala, R. K., & Lakshmanan, M. (2020). Experimental study on thermal management and performance improvement of solar PV panel cooling using form stable phase change material. *Energy Sources, Part A: Recovery, Utilization, and Environmental Effects*, *45*(1), 160–177. https://doi.org/10.1080/15567036.2020.1806409

[27] Nkwetta, Dan & Haghighat, Fariborz. (2014). Thermal energy storage with phase change material—A state-of-the art review. Sustainable Cities and Society. 10. 87–100. 10.1016/j.scs.2013.05.007. Pielichowski, Krzysztof & Njuguna, James & Majka, Tomasz. (2023). Modeling of thermal degradation processes. 10.1016/B978-0-12-823023-7.00008-3.

[28] Balasubramanian KR, Ravi Kumar K, Sathiya Prabhakaran SP, Jinshah BS, Abhishek N. Thermal degradation studies and hybrid neural network modelling of eutectic phase change material composites. Int J Energy Res. 2022; 46(11): 15733-15755. doi:10.1002/er.8272

[29] Hinojosa, J.F.; Moreno, S.F.; Maytorena, V.M. Low-Temperature Applications of Phase Change Materials for Energy Storage: A Descriptive Review. *Energies* **2023**, *16*, 3078. https://doi.org/10.3390/en16073078

[30] Rinderle, Michael; Kaiser, Waldemar; Mattoni, Alessandro; Gagliardi, Alessio (2020). Machine-Learned Charge Transfer Integrals for Multiscale Simulations in Organic Thin Films. ACS Publications. Collection. https://doi.org/10.1021/acs.jpcc.0c04355

[31] Abhishek S Chaudhary, Bandaru Kiran, K Sivagami, Dhivakar Govindarajan, Samarshi Chakraborty, Thermal degradation model of used surgical masks based on machine learning methodology, Journal of the Taiwan Institute of Chemical Engineers, Volume 144, 2023, 104732, ISSN 1876-1070, https://doi.org/10.1016/j.jtice.2023.104732.

[32] Yinzhou Liu, Weidong Zheng, Haoqiang Ai, Hao Zhou, Liyin Feng, Lin Cheng, Ruiqiang Guo, Xiaohan Song, Application of machine learning in predicting the thermal conductivity of single-filler polymer composites, Materials Today Communications, Volume 39, 2024, 109116, ISSN 2352-4928, https://doi.org/10.1016/j.mtcomm.2024.109116.

[33] Yogiraj Sargam, Kejin Wang, In Ho Cho, Machine learning based prediction model for thermal conductivity of concrete, Journal of Building Engineering, Volume 34, 2021, 101956, ISSN 2352-7102, https://doi.org/10.1016/j.jobe.2020.101956.

[34] Monticeli, F.M., Neves, R.M. & Ornaghi Júnior, H.L. Using an artificial neural network (ANN) for prediction of thermal degradation from kinetics parameters of vegetable fibers. *Cellulose* **28**, 1961–1971 (2021). https://doi.org/10.1007/s10570-021-03684-2

[35] Nurten Şahan, Halime Paksoy, Investigating thermal properties of using nano-tubular ZnO powder in paraffin as phase change material composite for thermal energy storage, Composites Part B: Engineering, Volume 126, 2017, Pages 88-93, ISSN 1359-8368, https://doi.org/10.1016/j.compositesb.2017.06.006.

[36] Patrik Sobolciak, Mustapha Karkri, Mariam A. Al-Maadeed, Igor Krupa, Thermal characterization of phase change materials based on linear low-density polyethylene, paraffin wax and expanded graphite, Renewable Energy, Volume 88, 2016, Pages 372-382, ISSN 0960-1481, https://doi.org/10.1016/j.renene.2015.11.056.

[37] Schulz, H. From the Kissinger equation to model-free kinetics: reaction kinetics of thermally initiated solid-state reactions. *ChemTexts* **4**, 9 (2018). https://doi.org/10.1007/s40828-018-0062-3

[38] B Eanest Jebasingh, A Valan Arasu, A comprehensive review on latent heat and thermal conductivity of nanoparticle dispersed phase change material for low-temperature applications, Energy Storage Materials, Volume 24, 2020, Pages 52-74, ISSN 2405-8297, https://doi.org/10.1016/j.ensm.2019.07.031.

[39] Abhay Lingayat, Pritam Das, Mulatu C. Gilago, Chandramohan V.P., A detailed assessment of paraffin waxed thermal energy storage medium for solar dryers, Solar Energy, Volume 261, 2023, Pages 14-27, ISSN 0038-092X, https://doi.org/10.1016/j.solener.2023.05.047.

[40] Aziz Babapoor, Gholamreza Karimi, Thermal properties measurement and heat storage analysis of paraffinnanoparticles composites phase change material: Comparison and optimization, Applied Thermal Engineering, Volume 90, 2015, Pages 945-951, ISSN 1359-4311, https://doi.org/10.1016/j.applthermaleng.2015.07.083.

[41] Jifen Wang, Huaqing Xie, Zhixiong Guo, Lihui Guan, Yang Li, Improved thermal properties of paraffin wax by the addition of TiO2 nanoparticles, Applied Thermal Engineering, Volume 73, Issue 2, 2014, Pages 1541-1547, ISSN 1359-4311, https://doi.org/10.1016/j.applthermaleng.2014.05.078.

[42] C.J. Ho, J.Y. Gao, Preparation and thermophysical properties of nanoparticle-in-paraffin emulsion as phase change material, International Communications in Heat and Mass Transfer, Volume 36, Issue 5, 2009, Pages 467-470, ISSN 0735-1933, https://doi.org/10.1016/j.icheatmasstransfer.2009.01.015.

[43] Kin Yuen Leong, Mohd Rosdzimin Abdul Rahman, Balamurugan A. Gurunathan, Nano-enhanced phase change materials: A review of thermo-physical properties, applications and challenges, Journal of Energy Storage, Volume 21, 2019, Pages 18-31, ISSN 2352-152X, https://doi.org/10.1016/j.est.2018.11.008.

[44] Liu, Yinzhou, Weidong Zheng, Haoqiang Ai, Hao Zhou, Liyin Feng, Lin Cheng, Ruiqiang Guo, and Xiaohan Song. "Application of machine learning in predicting the thermal conductivity of single-filler polymer composites." Materials Today Communications 39 (2024): 109116.

[45] Li, Wenbo, Zhang Tao, Yanqiang Liu, Zhiyu Yang, Ziyue Yang, Yabao Wang, Yu Ye, and Jianzhong Fan. "Graphene-based phase-change composites for thermal energy storage, conversion, and applications." Journal of Energy Storage 122 (2025): 116619.

[46] N. Pannucharoenwong, P. Rattanadecho, S. Echaroj, S. Hemathulin, and K. Nabudda, "The Experiment of Heat Absorber from Black Gasket on the Efficiency of Double Slope Solar Still," GMSARN International Journal, vol. 14, no. 1, pp. 1–10, 2020.